

Charge-dependent migration pathways for the Ga vacancy in GaAs

Fedwa El-Mellouhi*

*Département de physique and Regroupement québécois sur les matériaux de pointe, Université de Montréal,
Case Postale 6128, succ. Centre-ville, Montréal, Québec H3C 3J7, Canada*

Normand Mousseau†

Service de Recherches de Métallurgie Physique, Commissariat l'énergie atomique–Saclay, 91191 Gif-sur-Yvette, France

(Received 14 June 2006; revised manuscript received 4 October 2006; published 16 November 2006)

Using a combination of the local-basis *ab initio* program SIESTA and the activation-relaxation technique we study the diffusion mechanisms of the gallium vacancy in GaAs. Vacancies are found to diffuse to the second neighbor using two different mechanisms, as well as to the first and fourth neighbors following various mechanisms. We find that the height of the energy barrier is sensitive to the Fermi level and generally increases with the charge state. Migration pathways themselves can be strongly charge dependent and may appear or disappear as a function of the charge state. These differences in transition state and migration barrier are explained by the charge transfer that takes place during the vacancy migration.

DOI: [10.1103/PhysRevB.74.205207](https://doi.org/10.1103/PhysRevB.74.205207)

PACS number(s): 61.72.Ji, 71.15.Mb, 71.55.Eq, 71.20.Nr

I. INTRODUCTION

Self-diffusion is one of the basic mass-transport mechanisms in materials. While it is one of the most powerful tools used in the preparation of nanostructures,^{1–4} many questions remain regarding the microscopic details of self-diffusion. Recent studies have shown that even in the simplest cases, the mechanisms can be much more complicated than was initially thought. Diffusion on simple metallic surfaces, for example, was found to take place through a range of mechanisms involving from one to at least seven atoms.^{5,6} Similarly, recent studies on self-interstitial clusters^{7,8} and disordered systems^{9,10} have highlighted the importance of collective moves in easing atomic motion even in bulk systems, and underlined the importance of a detailed characterization of these mechanisms in materials of technological interest. This is the case for semiconductors, for example, which are at the heart of the electronics industry. While one predicts, using symmetry considerations, the self-diffusion pathways in elemental materials, such as silicon, this approach becomes impossible when impurities are added or multicomponent systems are considered. Thus, one must turn to experiments or numerical simulations to provide a direct and comprehensive study of diffusion mechanisms in semiconductors. The difficulty of extracting precise information on the diffusion mechanisms in these materials is compounded by the nature of bonding and the importance of charged defects which complicate seriously both experimental and theoretical studies.

Previous numerical studies of the migration pathways of intrinsic defects in binary semiconductors have focused on GaAs,¹¹ SiC,^{12,13} and GaN.¹⁴ Except in one case,¹¹ where high-temperature molecular dynamics was used, these works focus on optimizing preselected pathways using algorithms such as the drag¹¹ or the ridge method¹⁵ that rely on knowledge of the initial and final states in addition to a decent guess at the overall diffusion mechanism. While these approaches work efficiently to identify with precision the migration energy of previously known diffusion trajectories, they cannot help identify complex or unexpected mecha-

nisms that could also play an important role in the diffusion process.

Here, we present the application of the activation-relaxation technique in its more recent implementation (ART nouveau) to explore systematically the diffusion mechanisms of complex systems. More precisely, we focus on the diffusion of V_{Ga} in GaAs because of its apparent simplicity but also because of its technological interest and its role in affecting the properties of bulk materials and nanostructures. Gallium vacancies are found to be mobile at typical growth and annealing temperatures¹⁶—with a dominant charge state strongly depending on growth conditions, temperature, dopants, etc.—playing the main role in dopant diffusion. For example, Bracht *et al.*¹⁷ showed recently that the contribution of V_{Ga} to Ga self-diffusion in GaAs is even more important than in earlier estimations, giving an important contribution to the total diffusion profile. Furthermore, Tuomisto *et al.*¹⁸ found that Ga vacancies play a central role in the migration of Mn in $\text{Ga}_{1-x}\text{Mn}_x\text{As}$ alloys. Finally, the energy blueshift in photoluminescence spectra of $\text{In}_x\text{Ga}_{1-x}\text{As}/\text{GaAs}$ (Ref. 19) and $\text{InAs}/\text{Ga}_x\text{In}_{1-x}\text{P}$ quantum dots²⁰ has also been recently attributed to V_{Ga} diffusion.

Focusing on a simple defect, a gallium vacancy (V_{Ga}), in the weakly ionic GaAs, we show here that diffusion in bulk semiconductors is a complex phenomenon that depends not only on the geometry of the defect and the surrounding lattice but also on its charge. In particular, we identify a previously unrecognized mechanism for the diffusion to the second neighbor in addition to the one already found by Bockstedte and Scheffler,¹¹ plus a number of other jumps to the first and fourth neighbors. Not all these pathways are likely to occur in a normal range of temperatures, and some exist only for a subset of charge states, but their existence underlines the underestimated richness of diffusion mechanisms in bulk materials.

This paper is organized as follows. In Sec. II, we present the details of activated event generation using SIESTA-RT. A description of initial and different transition states in various charge states is presented in Sec. III. In Sec. IV we discuss

the origin of the charge-dependent migration barrier and we compare our results with experimental and theoretical works.

II. DETAILS OF THE SIMULATION

Our simulations are performed using SIESTA-RT, a method combining a self-consistent density functional method code²¹ (SIESTA) with the most recent version of the activation relaxation technique (ART nouveau).²² Integrating various empirical potentials, ART nouveau was shown to sample efficiently the energy landscape of amorphous semiconductors,²³ glasses,²² and proteins,²⁴ for example.

SIESTA-RT was used for the first time to study vacancy diffusion in Si and details of its implementation can be found in Ref. 25. Forces and energies are evaluated using density-functional theory (DFT) with the local-density approximation (LDA) using standard norm-conserving pseudopotentials of Troullier and Martins²⁶ factorized in the Kleinman-Bylander form.²⁷ Matrix elements are evaluated on a three-dimensional (3D) grid in real space. The one-particle problem is solved using a linear combination of pseudo-atomic orbitals (PAOs) basis set of finite range. Here, we use the extended local basis set,²⁸ which was shown to reproduce closely the best solution while minimizing computational costs. Calculations are performed on a 215-atom GaAs supercell sampled at the Γ special point. All relevant charge states (0, -1, -2, and -3) are fully relaxed until the residual force falls below 0.002 eV/Å; then we proceed to search for local diffusion pathways by assuming that the charge state of the defect is preserved during any transformation. Unless mentioned, all events start from fully relaxed gallium vacancy geometries.

In order to break the initial local symmetry, activated events are started by displacing in a random direction a region of the cell centered around a chosen atom in the first, second, or fourth shell around the vacancy, involving typically between 10 and 30 atoms. The structure around the vacancy is then deformed along this random direction until the lowest curvature, corresponding to the lowest eigenvalue of the Hessian matrix, becomes negative, falling below a preset threshold value. The system is then pushed along the corresponding eigenvector, while minimizing the energy in the perpendicular hyperplane, until the total force falls below 0.1 eV/Å, indicating that the transition state has been reached.

About 60 events were generated in total for all charge states, with 20 events for jumps to the first nearest neighbor and 30 for jumps to the second neighbor. In both cases the structure is deformed by at least 0.9 Å before a sufficiently negative eigenvalue appears. Diffusion to the fourth neighbor was more difficult to complete (we generated ten such events in total) and we set up a threshold displacement of 1.4 Å to allow the configuration to escape from the harmonic well.

III. RESULTS

A. Gallium vacancies at the initial state

We first examine the vacancy at the initial state before moving to the analysis of transition states. The structure of

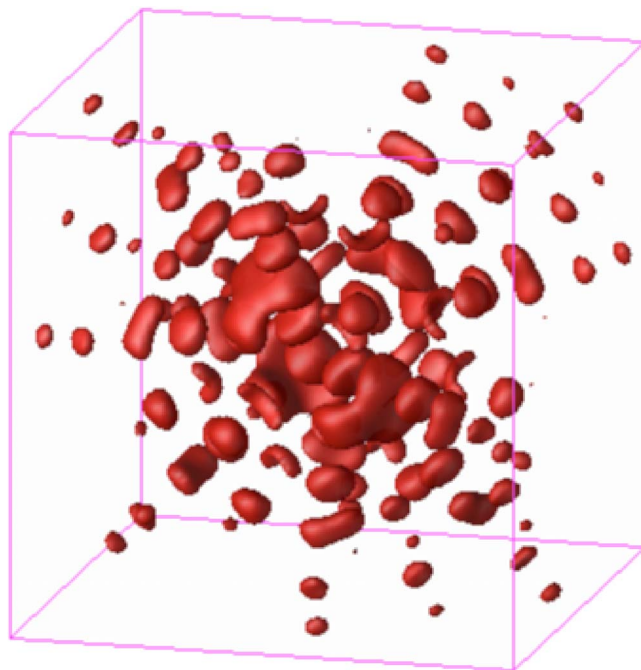


FIG. 1. (Color online) Constant surface at 0.0004 electron/Å³ of the difference in electronic charge density between the neutral and the -3 charged gallium vacancies. The gallium vacancy is located initially at the center of the box.

V_{Ga} for all charge states, for a number of basis sets within SIESTA, is presented in Ref. 28 and agrees well with results of other simulations and experiments. Relaxed at its energy minimum, V_{Ga} conserves the T_d symmetry for all charges, while the open volume associated with the vacancy decreases with increasing charge. Spin-polarized LDA relaxations for V_{Ga} also lead to a T_d symmetry, confirming that the symmetry conservation of V_{Ga}^q is not a drawback of the LDA but a behavior proper to cation vacancies, as pointed out previously by Chadi.²⁹ This behavior has been further confirmed by a recent calculation³⁰ on V_{Ga} in GaAs using the two-component density-functional theory LDA applied to a cubic 64-atom supercell together with a 4^3 k -point mesh Brillouin zone sampling.

A detailed analysis of the charge density plots (see Fig. 1) and the Mulliken populations reveals that the electrons added to the neutral vacancy are delocalized and distribute themselves on the 111 axes passing by the As dangling bonds in a similar way for all studied charge states. Less than 4% of the charge is localized on the four As neighbors the vacancy ($\text{As}^{1\text{st}}$) while the remaining 96% is spread over more distant neighbors on the 111 axes. This suggests that these predominantly covalent As-Ga bonds are progressively stiffened upon the addition of extra electrons, thus making them more difficult to break compared to the remaining bonds, and affecting directly the height of the diffusion barriers.

B. Diffusion path to first neighbor

The activated events we generated using SIESTA-RT show that diffusion to the first nearest neighbor is not possible for

TABLE I. Nearest neighbor distances (in Å) in 111 direction relevant for first nearest neighbor diffusion from the initial to the final state. Distances are calculated by taking the initial position of V_{Ga} as reference. The last column describes the geometry of the final state.

	$V_{\text{Ga}}\text{-As}^{1\text{st}}$	$\text{As}^{1\text{st}}\text{-Ga}^{2\text{nd}}$	$\text{Ga}^{2\text{nd}}\text{-As}^{3\text{rd}}$	Final geometry
V_{Ga}^0	2.08 → 0.44	2.43 → 3.40	2.45 → 2.46	$(\text{As}_{\text{Ga}} + V_{\text{As}}^{1\text{st}})^0$
V_{Ga}^{-1}	2.08 → 0.90	2.42 → 2.65	2.45 → 2.58	$(V_{\text{Ga}} + I_{\text{As}} + V_{\text{As}}^{1\text{st}})^{-1}$
V_{Ga}^{-2}	2.06 → 0.53	2.41 → 2.69	2.45 → 2.64	$(\text{As}_{\text{Ga}} + V_{\text{As}}^{1\text{st}} + I_{\text{Ga}} + V_{\text{Ga}}^{2\text{nd}})^{-2}$
V_{Ga}^{-3}	Do not diffuse to the first neighbor			

all sequential charge states, contrary to what was proposed by Van Vechten,³¹ nor impossible, in contradiction with what was found by Bockstedte and Scheffler.¹¹ We find rather that diffusion to the first nearest neighbor is very much charge dependent.

For $q=0$ the first neighbor of the vacancy ($\text{As}^{1\text{st}}$) diffuses, along the 111 direction, toward the vacant site via a split vacancy configuration by optimizing its bonds with the close neighbors. This mechanism is similar to the diffusion mechanism of a neutral silicon vacancy in silicon.^{25,32,33} First, each back bond of the diffusing atom ($\text{As}^{1\text{st}}\text{-Ga}^{2\text{nd}}$) stretches until it breaks during the migration of $\text{As}^{1\text{st}}$ toward the vacancy. $\text{As}^{1\text{st}}$ proceeds in its migration until a metastable vacancy-antisite structure ($\text{As}_{\text{Ga}} + V_{\text{As}}^{1\text{st}}$) forms. The $\text{As}^{1\text{st}}\text{-Ga}^{2\text{nd}}$ bond evolves from 2.43 Å at the initial state to 3.40 Å at the final state. This metastable complex is 0.67 eV higher than V_{Ga} and the recorded migration barrier for the first neighbor diffusion is 0.84 eV. The next first neighbor jump ($V_{\text{As}}^{1\text{st}} \rightarrow \text{Ga}^{2\text{nd}}$) leading to the formation of the $\text{As}_{\text{Ga}} + \text{Ga}_{\text{As}}^{1\text{st}} + V_{\text{Ga}}^{2\text{nd}}$ complex is also possible by crossing a barrier of 1.55 eV. Starting from this last complex we did not find any mechanism for $V_{\text{Ga}}^{2\text{nd}}$ to diffuse further to the first neighbor, suggesting that this jump is unfavorable.

For $q=-1$ the vacancy follows the same path to the saddle point as for $q=0$: it crosses a barrier of 0.9 eV passing by a split vacancy site, but $\text{As}^{1\text{st}}\text{-Ga}^{2\text{nd}}$ bond is less stretched. $\text{As}^{1\text{st}}$ relaxes then in a split vacancy site, forming a $(V_{\text{Ga}} + I_{\text{As}} + V_{\text{As}}^{1\text{st}})^{-1}$ complex. The $\text{As}^{1\text{st}}\text{-V}_{\text{Ga}}$ distance is reduced to half (2.08 Å → 0.90 Å) suggesting that $\text{As}^{1\text{st}}$ is halfway between the two vacancies. This metastable configuration is 0.81 eV higher than the initial minimum. We confirmed that this final metastable state is not only a local minimum along the diffusion path to the first neighbor by starting from an ideal vacancy-antisite complex ($\text{As}_{\text{Ga}} + V_{\text{As}}^{1\text{st}}$), then relaxing until the residual force becomes lower than 0.002 eV/Å. This vacancy-antisite structure is found to be unstable in the -1 charge state because $\text{As}^{1\text{st}}$ leaves the ideal antisite structure and prefers to relax at a metastable state halfway between the two vacancies.

For $q=-2$, we find only a collective motion of a $\text{As}^{1\text{st}}\text{-Ga}^{2\text{nd}}$ pair toward the vacancy along the 111 direction. The $\text{As}^{1\text{st}}\text{-Ga}^{2\text{nd}}$ bond stretches slightly, while $\text{As}^{1\text{st}}$ approaches V_{Ga}^{-2} as close as 0.53 Å. Consequently, $\text{Ga}^{2\text{nd}}$ is forced to stretch its back bonds and stabilizes in an interstitial position. Finally, the $\text{As}^{1\text{st}}$ atom occupies V_{Ga} while $\text{Ga}^{2\text{nd}}$ is located at a split interstitial position between $V_{\text{As}}^{1\text{st}}$ and $V_{\text{Ga}}^{2\text{nd}}$. The resulting metastable complex $(\text{As}_{\text{Ga}} + V_{\text{As}}^{1\text{st}} + I_{\text{Ga}} + V_{\text{Ga}}^{2\text{nd}})^{-2}$ is 1.74 eV

higher in energy than V_{Ga}^{-2} and can be obtained by crossing a barrier of 1.86 eV. Relevant distances for successful first nearest neighbor diffusion in $q=0, -1, -2$ are summarized in Table I.

For $q=-3$, all attempts for first nearest neighbor diffusion failed and the configuration always relaxes back to the initial minimum. Even when the jump is forced by using the transition state at the neutral charge state as starting point for a convergence of the V_{Ga}^{-3} to its saddle point, the vacancy systematically returns to its original state.

C. Diffusion path to fourth neighbor

The situation is almost opposite for the diffusion to the fourth neighbor: all negatively charged vacancies succeed in diffusing along this pathway; only the neutral vacancy refuses to go this way.

The fourth neighbor of the vacancy ($\text{Ga}^{4\text{th}}$) approaches the interstitial region near the vacancy by diffusing along the 100 direction. Figure 2 illustrates this configuration: the dashed arrow shows the direction of the jump from the initial state to the saddle point, while the full arrow shows the path from the saddle to the final. $\text{Ga}^{4\text{th}}$ diffuses to an unstable

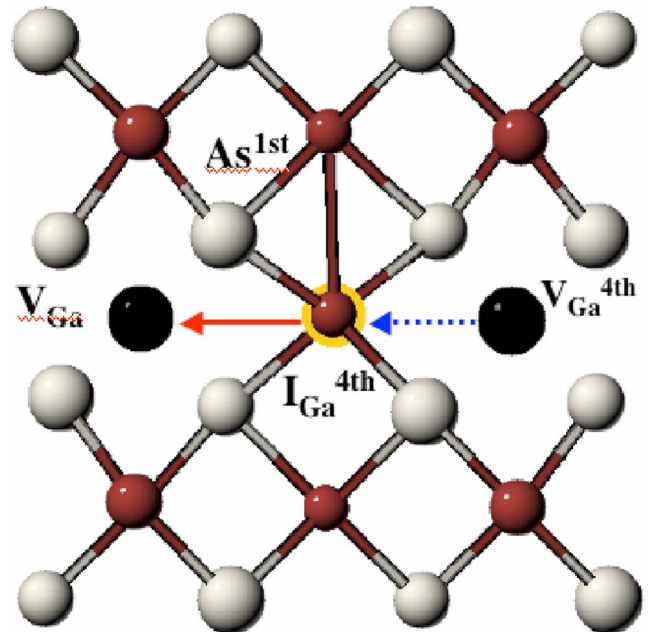


FIG. 2. (Color online) Migration path of V_{Ga}^q to the fourth neighbor along (100) direction (see the text).

interstitial position close to the vacancy. In the cubic zincblende structure of GaAs, with lattice constant a and a vacancy located initially at $(0,0,0)$, the fourth neighbor diffuses first from $(a,0,0)$ to the interstitial position at $(a/2,0,0)$. The transition state of this mechanism can be described as a gallium interstitial placed between two distant vacancies ($V_{\text{Ga}}-I_{\text{Ga}}^{\text{4th}}-V_{\text{Ga}}^{\text{4th}}$). This interstitial atom is not a direct neighbor of either of the two vacancies because the $\text{Ga}^{\text{4th}}-V_{\text{Ga}}$ distance shortens from 5.6 Å at the initial minimum to 2.88 Å at the transition state. This diffusion mechanism requires an elevated barrier (around 4.24 eV) since the Ga^{4th} needs to break two bonds initially with As^{5th} farthest away from the vacancy and to twist the remaining As^{3rd} bonds. Once it arrives at the saddle point two new bonds with As^{1st} are formed. It is interesting to note, as shown in Table III below that the energy barrier is almost independent of the charge for the defects that manage to diffuse to the fourth neighbor; this weak dependence can probably be attributed to the constant electronic charge distribution along the 100 direction for different negative charging.

D. Diffusion path to second neighbor

By exploring the energy landscape of the system, we find that vacancy migration to the second neighbor occurs by two mechanisms. The simplest diffusion pathway is already well known¹¹ and is considered to mediate self-diffusion in binary semiconductors, while the second pathway, which has not been reported, to our knowledge, for this system, is more complex and involves the correlated motion of many atoms neighboring the vacancy.

1. Plane-passing mechanism

The most intuitive diffusion pathway, which we call the *plane-passing mechanism*, brings one Ga^{2nd} to the interstitial region, joining the diffusing atom and the vacancy, along the 110 direction. The diffusing Ga^{2nd} atom must go through the diffusion plane perpendicular to the 110 direction during its way to the vacancy site causing three As^{1st} atoms to move away from the vacancy and opening the cage. The transition state of this mechanism, first identified by Bockstedte and Scheffler,¹¹ can be described as a gallium interstitial placed between two close vacancies ($V_{\text{Ga}}+I_{\text{Ga}}^{\text{2nd}}+V_{\text{Ga}}^{\text{2nd}}$). Figure 3 illustrates this configuration: the dashed arrow shows the direction of the jump from the initial state to the saddle point, while the full arrow shows the path from the saddle to the final; the diffusion plane formed by the second nearest neighbors of the vacancy is also shown.

From Table II, it is clear that, as with the other mechanisms to first and fourth neighbors, the structural details of the jumps are charge dependent. The position of the transition state, in particular, changes by 20% as the vacancy goes from neutral to a charge of -3 . As can be expected, the displacement of the unstable interstitial position as the diffusing atom becomes a nearest neighbor of the vacancy has noticeable impact on the energy barrier, which goes from 1.7 eV for the neutral and -1 charge states to 1.84 and 2.0 eV for -2 and -3 charges, respectively.

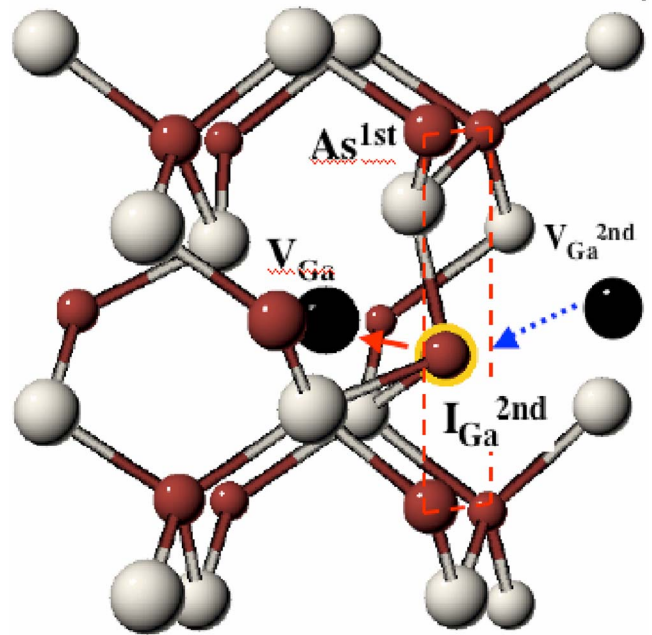


FIG. 3. (Color online) Diffusion to second neighbor by plane-passing mechanism (refer to the text).

More precisely, for V_{Ga}^0 and V_{Ga}^{-1} , the saddle point is a site close the hexagonal interstitial, while it is closer to the tetrahedral interstitial configuration for the more negative V_{Ga}^{-2} and V_{Ga}^{-3} . At the transition state, as the charge increases, the displacement of the gallium atom out of the plane becomes less pronounced; for the -3 charge state, it almost vanishes, leaving the moving atom on the plane.

This can be seen by looking at the full migration trajectory for the -3 charge state in Fig. 4. This path is generated by initially interpolating between the ART-generated initial, saddle, and final states, generating 11 images. These image configurations are then relaxed using the climbing-image (CI) nudged-elastic-band method³⁴ (NEBM) until the total force becomes lower than 1 eV/Å. After decomposing the total path into contributions coming from different moving atoms one can notice that the path followed by the diffusing atom is nearly symmetric, while most asymmetry in the total path comes from the arrangement of the other atoms around the defect.

Differences in the migration barriers are mainly due to the diffusion of the electronic charge during the jump. For the

TABLE II. Evolution of the distance (in Å) between the initial position of the vacancy and the diffusing atom ($V_{\text{Ga}}^q-\text{Ga}^{\text{2nd}}$) in the initial state and the transition state for both diffusion mechanisms to the second neighbor.

	Plane passing		Cluster assisted	
	Initial	Saddle	Initial	Saddle
V_{Ga}^0	3.89	1.89		
V_{Ga}^{-1}	3.88	2.09	3.88	2.5
V_{Ga}^{-2}	3.82	2.19	3.82	2.78
V_{Ga}^{-3}	3.80	2.35	3.80	2.89

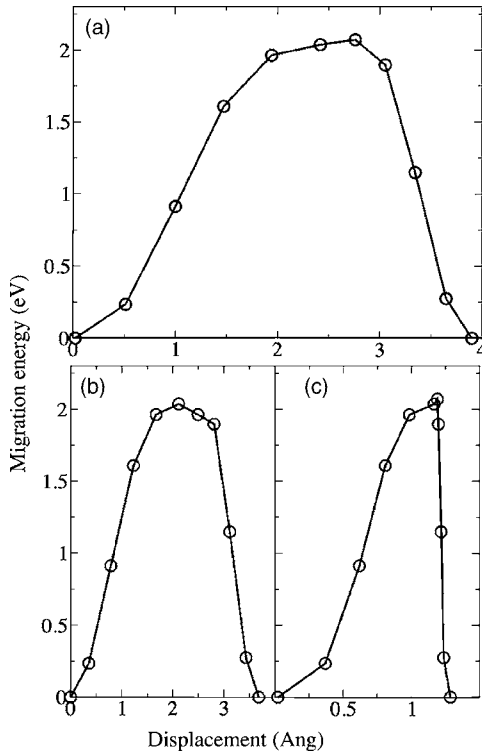


FIG. 4. (a) Migration trajectory to the second neighbor by the plane-passing mechanism for -3 charge state. 11 images (circles) are relaxed with the CI NEB method until a force tolerance of 1 eV/\AA is reached; lines are guides to the eye. The contributions from different moving atoms are decomposed into two: (b) the path followed by the diffusing atom; (c) arrangement of the other atoms around the defect.

singly negative vacancy, Mulliken population analysis at the saddle point (top panel in Fig. 5) is compared to the initial configuration. It shows the diffusion of the electronic charge during the migration of the $\text{Ga}^{2\text{nd}}$ atom. The electronic charge at $\text{Ga}^{2\text{nd}}$ diffuses with it to the hexagonal interstitial site thus saturating partially the $\text{As}^{1\text{st}}$ dangling bonds. The charge is consequently suppressed from the neighborhood of the diffusing atom ($I_{\text{Ga}}^{2\text{nd}}$) and spreads uniformly over more distant shells as can be seen from the 3D charge density (top inset of Fig. 5).

For $V_{\text{Ga}}^{2,-3}$ the diffusing atom is less engaged toward the vacancy: circles in the lower panel in Fig. 5 are shifted to the right as a signature of volume opening that affects the second neighbor of the vacancy as well. However, the 3D charge densities for $V_{\text{Ga}}^{2,-}$ and $V_{\text{Ga}}^{3,-}$ are different from that of $V_{\text{Ga}}^{1,-}$. After the jump, the charge becomes highly localized around the dangling bonds belonging to As atoms farthest away from $I_{\text{Ga}}^{2\text{nd}}$, labeled $\text{As}^{1\text{st far}}$. Some of the charge carried by two closer $\text{As}^{1\text{st close}}$ to $I_{\text{Ga}}^{2\text{nd}}$ get transferred to the other $\text{As}^{1\text{st far}}$; these have non saturated bonds that are still pending.

2. Cluster-assisted mechanism

Negatively charged V_{Ga} can also diffuse on the Ga sublattice through a mechanism that we call the *cluster-assisted path*. As far as we know, this diffusion pathway had not been reported until now. Instead of crossing the diffusion plane

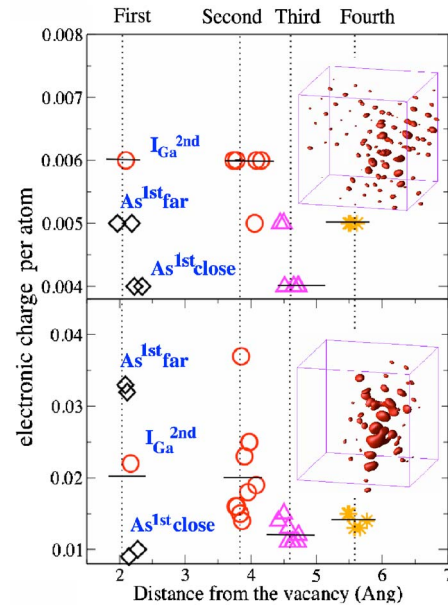


FIG. 5. (Color online) Mulliken population analysis of the difference in electronic charge between the neutral and the -1 (upper panel) and -3 (lower panel) charge states at the saddle point of the plane-passing mechanism as a function of the distance from the center of the vacancy. The insets show these charge densities in 3D at 0.00018 and 0.0008 electron/ \AA^3 near V_{Ga}^{-1} and V_{Ga}^{-3} , respectively. The charge transfer during the plane-passing path could be deduced by comparing the initial and the saddle point populations: Mulliken populations at the initial state are indicated by horizontal solid lines, vertical dotted lines indicate the positions of the first, second, third, and fourth neighboring shells of the vacancy. At the saddle point, populations for each of the atoms originating from the first arsenic (\diamond), second gallium (\circ), third arsenic (\triangle), and fourth gallium shells ($*$) are shown.

directly, $\text{Ga}^{2\text{nd}}$ approaches the interstitial region far from the plane, being assisted by two As atoms—respectively first ($\text{As}^{1\text{st}}$) and third neighbors ($\text{As}^{3\text{rd}}$) of the vacancy—and one gallium atom second neighbor of the vacancy, $\text{Ga}^{2\text{nd}}$. From the initial to the transition state (dashed arrows in Fig. 6), an incomplete bond exchange mechanism of Wooten-Winer-Weaire type³⁵—which we also find in Si—occurs between $\text{Ga}^{2\text{nd}}$ and $\text{As}^{3\text{rd}}$, then $\text{Ga}^{2\text{nd}}$ is pushed into the interstitial region.

The cluster formed by $\text{As}^{1\text{st}} + I_{\text{Ga}}^{2\text{nd}} + \text{As}^{3\text{rd}} + \text{Ga}^{2\text{nd}}$ plays the major role for diffusion since the bond distances $I_{\text{Ga}}^{2\text{nd}} - \text{As}^{1\text{st}}$ and $I_{\text{Ga}}^{2\text{nd}} - \text{As}^{3\text{rd}}$ remain unchanged (2.4 \AA) regardless of the charge state, while the $V_{\text{Ga}}^q - I_{\text{Ga}}^{2\text{nd}}$ distance increases by adding extra electrons (see Table II). This assumes that the whole cluster becomes less engaged toward the vacancy when passing from -1 to -3 charge states. During the relaxation from the saddle point to the final state (full arrow in Fig. 6) only the gallium atom at the interstitial position ($I_{\text{Ga}}^{2\text{nd}}$) continues its motion toward the vacancy, leaving the remaining constituents of the cluster close to their initial positions. This is confirmed by looking at the full migration trajectory for the -3 charge state for the cluster-assisted mechanism plotted in Fig. 7. From the initial to the saddle point many atoms are experiencing rearrangements and displacements, but the

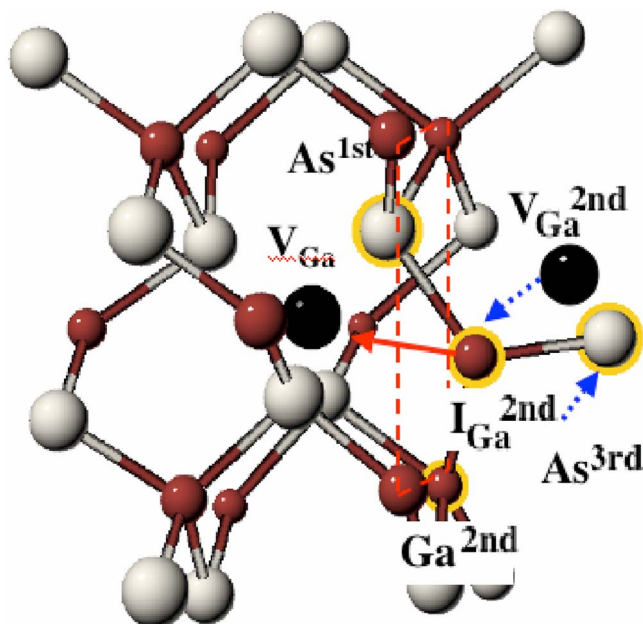


FIG. 6. (Color online) Diffusion to second neighbor by cluster-assisted mechanism (refer to the text).

main contribution comes from the diffusing atom, which is less engaged toward the vacancy than for the plane-passing mechanism, while during the relaxation from the saddle point to the final state the main contribution to the total path comes from the relaxation of the $I_{\text{Ga}}^{2\text{nd}}$ atom [Fig. 7(b)].

Mulliken population analysis shows that the electronic charge diffusion for the cluster-assisted mechanism is completely different from that of the plane-passing mechanism. By increasing the charge state of the vacancy from -1 to -3 , the positions of the cluster atoms are all shifted to the right, confirming that the whole cluster is experiencing a displacement far away from the vacancy. In addition, the electronic charge becomes more and more concentrated around the cluster as the charge on the defect increases. Consequently, the migration barrier increases in a significant way with the charge state reaching 2.44, 2.89, and 3.24 eV for -1 , -2 , and -3 charges, respectively.

No cluster-assisted path was found at the neutral state: we tried to generate this event by starting directly from the transition state at -1 charge, but the neutral vacancy relaxes back to the initial minimum rather than diffuse to the second neighbor site, demonstrating that this path is impossible in the neutral charge state.

E. Summary of the results

The summary of the calculated migration barriers is presented in Table III. While these migration barriers are calculated with a 216-atom supercell using the Γ point, we have checked that these values are stable by further relaxing some of them with a $2 \times 2 \times 2$ Monkhorst-Pack k -point mesh. This additional relaxation does not change the structure or the energies of these barriers.

First neighbor diffusion has the lowest barrier for 0 and -1 charges, but cannot be considered to be dominant for V_{Ga}

TABLE III. Calculated diffusion barriers (in eV) for $V_{\text{Ga}}^{0,-1,-2,-3}$ in GaAs for all possible migration paths identified. The empty cell means that the migration was not possible with this mechanism.

	V_{Ga}^0	V_{Ga}^{-1}	V_{Ga}^{-2}	V_{Ga}^{-3}
First neighbor	0.84	0.90	1.86	
Plane passing	1.7	1.7	1.84	2.0
Cluster assisted		2.44	2.89	3.24
Fourth neighbor		4.24	4.24	4.3

since the complete diffusion process is impossible to achieve even for the neutral vacancy. However, this mechanism induces the formation of defects belonging to the As_{Ga} family. These antisite defects are of great importance since they are responsible for EL-type defects in GaAs (see the discussion below).

Self-diffusion will rather be dominated by jumps to the same sublattice. Gallium vacancies can diffuse to the second neighbor through the plane-passing mechanism for all charge states by crossing barriers lower than 2 eV. The impact of the charge state on the trajectory is reflected on the charge-dependent barrier-height energy; for example, the barrier height for V_{Ga}^{-3} is 18% higher than for V_{Ga}^0 , making the crossing 30 times less likely at 1000 K. The simplicity of this path

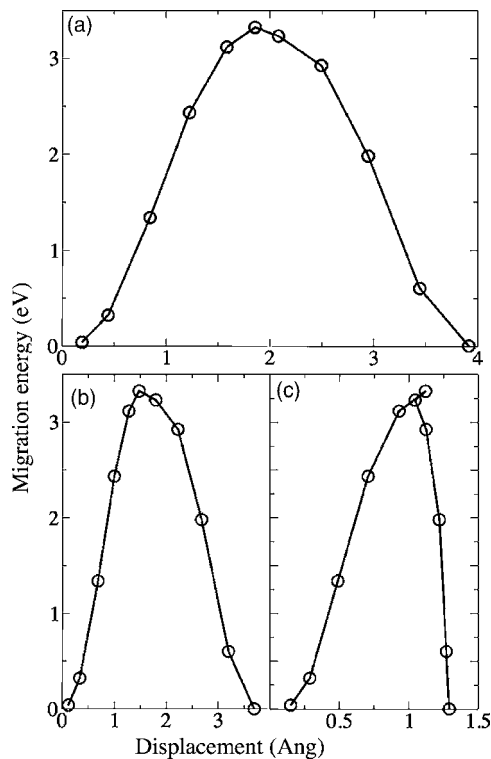


FIG. 7. (a) Migration trajectory to the second neighbor by the cluster-assisted mechanism for -3 charge state. 11 images (circles) are relaxed with the CI NEB method until a force tolerance of 1 eV/\AA is reached; lines are guides to the eye. The contributions from different moving atoms are decomposed into two: (b) The path followed by the diffusing atom; (c) arrangement of the other atoms around the defect.

as well as the relatively low migration barrier make the plane-passing mechanism the potential candidate to mediate vacancy self-diffusion in GaAs.

Negatively charged vacancies might also follow the cluster-assisted pathway to diffuse to the second neighbor or diffuse directly to the fourth neighbor with energy barriers that are by about 50% and 100%, respectively, higher than that of the plane-passing mechanism. Although these two mechanisms have elevated barriers, their existence is very interesting by itself as it shows the underestimated richness of self-diffusion phenomena in bulk semiconductors.

IV. DISCUSSION AND COMPARISONS

A. Self-diffusion to first neighboring sites

In a binary lattice, vacancy hops to the first-neighbor sites require a complex sequence of moves to preserve chemical ordering on the long run. In 1984, Van Vechten³¹ proposed a model leading to vacancy diffusion to the second neighbor in GaAs. His model describes a 11 first neighbor hop process on a six-membered ring and is based on two assumptions: (i) jumps to the first neighbors are always possible, and (ii) vacancy-antisite complexes are always stable. During successive hops the vacancy should proceed, leaving behind a chain of antisites, which is energetically unfavorable. This is avoided by the vacancy passing twice through the same six-fold ring. At the final stage all the antisite defects are removed. Otherwise such a mechanism would create an unfavorable excess of antisite defects beyond the equilibrium concentration. Bockstedte and Scheffler¹¹ studied the validity of these assumptions—possible diffusion via first neighbor hops—using the drag method and the LDA. They found that $\text{As}_{\text{Ga}} + V_{\text{As}}^{\text{1st}}$ is metastable in the neutral state while it is unstable for other negative charge states for a 64-GaAs-atom system. They concluded that diffusion by first nearest neighbor hops was impossible.

Our study shows that the complex is rather metastable in the -1 charge state too. The first nearest neighbor diffusion of V_{Ga} in -1 and -2 charge states is found to be possible via *deformed* structures belonging to the As_{Ga} family. While V_{Ga} diffusion to the first neighbor leads to a symmetric $\text{As}_{\text{Ga}}-V_{\text{As}}$ complex in the neutral state, this configuration is distorted in the case of -1 charge states. In the deformed structure for the -1 charge state, As atoms do not occupy the tetrahedral gallium vacancy site; rather they are displaced from the Ga vacancy site by about 0.9 eV toward $V_{\text{As}}^{\text{1st}}$. Interestingly, this deformed structure is no longer metastable for -2 ; the transition state originates from an $\text{As}_{\text{Ga}} + \text{Ga}_{\text{As}} + V_{\text{Ga}}$ complex, with Ga_{As} pushed toward V_{Ga} and occupying a split vacancy site.

We attribute this charge-dependent first neighbor diffusion to two competing factors: (1) the progressive increase in the strength of $\text{As}^{\text{1st}}-\text{Ga}^{\text{2nd}}$ bonds as electrons are added make them more difficult to break, and (2) the electron density in the region surrounding the vacancy—especially on As dangling bonds—increases as electrons are added to the relaxed system. Thus, Coulomb repulsion between three As^{1st} atoms and the diffusing As^{1st} atom can become so strong that this atom cannot approach the vacant site further. This picture

causes the As^{1st} atom to relax at the split vacancy configuration in the -1 charge state. If the system is charged -2 , the $\text{As}^{\text{1st}}-\text{Ga}^{\text{2nd}}$ bond is so strong that As^{1st} pulls Ga^{2nd} with it during its diffusion to the saddle point position, leaving behind $V_{\text{As}}^{\text{1st}}$ and $V_{\text{Ga}}^{\text{2nd}}$. The electronic density is partially transferred from the initial vacancy to these two new vacancies, allowing As^{1st} to relax on the initial vacant site and leaving the Ga^{2nd} atom stacked between $V_{\text{As}}^{\text{1st}}$ and $V_{\text{Ga}}^{\text{2nd}}$.

Similarly deformed structures for negatively charged defects have been recently reported in the literature. Chadi³⁶ found that the isolated As antisite structure (As_{Ga}) is generally accepted to be the basic structure of the EL2 defect) exists in charge states $+2$, $+1$, and 0 , occupying the tetrahedrally symmetric position, and in -1 , -2 charge states when it undergoes a small displacement that causes a deviation from T_d symmetry. The main difference between the different charge states is the degree of relaxation that the antisite and its direct neighbor undergo. This possible high negative charging of As_{Ga} inducing a structural relaxation is similar to the deformed negatively charged $\text{As}_{\text{Ga}}-X$ observed in this work.

Moreover, the electronic structure of $\text{As}_{\text{Ga}}-V_{\text{As}}$ has been studied by total-energy Green's-function calculations treating many-body effects within LSDA DF,³⁷ and shows that the electronic levels allow at most -1 charging for this complex, which is in agreement with our results.

On the experimental side, negatively charged $V_{\text{As}}-X$ complexes have been recently detected by positron annihilation experiments³⁹ between 20 and 330 K in weakly *p*-type GaAs under arsenic-rich conditions. The detection of $V_{\text{As}}-X$ complexes in these samples was surprising and not previously reported, since under these conditions²⁸ isolated arsenic vacancies are unlikely to form. V_{Ga} diffusion to the first neighbor after annealing could explain these findings, assuming that the metastable complex $\text{As}_{\text{Ga}}-V_{\text{As}}$ could be detected at sufficiently low temperatures.

In addition, $\text{As}_{\text{Ga}}-V_{\text{As}}$ structure was proposed by Steinegger *et al.*³⁸ to be a potential candidate for the EL6 defect. Measuring the relative concentration of EL6 by photon-induced current-transient spectroscopy at room temperature, they observed an increase of As_{Ga} concentration with annealing time by roughly a factor of 2 corresponding to a decrease of V_{Ga} concentration from about 10^{16} to zero. While the first nearest neighbor diffusion cannot play a role in self-diffusion, we suggest that it is dominant in these conditions, leading to the transformation of a large number of V_{Ga} into $\text{As}_{\text{Ga}}-V_{\text{As}}$ complexes.

B. Diffusion to second neighbor

Nevertheless, diffusion to the second neighbor is more interesting since it conserves the equilibrium concentration of vacancies. The plane-passing paths of V_{Ga} simulated with SIEST-A-RT confirm that the transition state does cross the diffusion plane in all charge states. For all our simulations the As^{1st} atom crosses the plane before the Ga^{2nd} atom; we did not record any event where As^{1st} crossed the plane or where it was located on the plane as suggested by Bockstedte and Scheffler.¹¹ However, the presence of the extra charge affects the diffusion trajectory by increasing the distance be-

tween the moving atom ($\text{Ga}^{2\text{nd}}$) and the three $\text{As}^{1\text{st}}$ dangling bonds. For V_{Ga}^{-2} and V_{Ga}^{-3} the charge on $\text{As}^{1\text{st}}$ is so strong that it scatters the moving atom and pushes it away from the vacancy toward the plane. Consequently, the distance between the plane and the atom is lowered as the charge of the vacancy increases; it almost vanishes for the -3 charge state.

The diffusion barrier of the plane-passing mechanism is found to increase moderately as extra electrons are added. Recent theoretical works reported a charge-dependent migration to the second neighbor by the plane-passing mechanism for vacancies in SiC and GaN binary semiconductors. Bockstedte *et al.*¹² found that the migration barrier for diffusion of V_{C} and V_{Si} in 4C-Si decreases when the vacancy charges are increasing progressively. A similar trend was observed¹⁴ for V_{N} in GaN and recently for V_{Ga} in GaN.⁴⁰ Our most recent results with SIESTA-RT concerning⁴¹ V_{As} in GaAs suggest that the migration barrier in the plane-passing mechanism decreases on progressively increasing the vacancy charging. Thus, V_{Ga} in GaAs shows an opposite trend compared to previously studied vacancies. This trend was observed previously by Bockstedte and Scheffler¹¹ as they found a migration barrier of 1.7 eV for neutral and 1.9 eV for the -3 charge state. This behavior cannot be a drawback of SIESTA-RT, since the total path relaxed using CI NEBM led to the same barrier; it is rather correlated with the electronic charge diffusion of V_{Ga} in GaAs.

Experimentally, negatively charged gallium vacancy migration on a GaAs(110) surface has been found to be stimulated by the tip during STM experiments⁴² only when holes are injected on the surface, consequently reducing the negative charging of the vacancy. This supports our results suggesting that the migration barrier is lowered as the vacancy becomes less negatively charged.

C. Diffusion in experimental systems

Bliss *et al.*⁴³ identified the migration barriers for V_{Ga} in low-temperature GaAs by the positron annihilation technique. They found a migration enthalpy of 1.5 ± 0.3 eV for the vacancy diffusion to the second neighbor and 1.1 ± 0.3 eV for diffusion to the first neighbor. Within the experimental error bars, these results agree with our calculated barriers summarized in Table III. Our results are also consistent with the widely accepted value of 1.7–1.8 eV for GaAs vacancy migration in bulk and GaAs-based quantum well materials.^{44–48} This value has been recently reported for interdiffusion in $\text{In}_x\text{Ga}_{1-x}\text{As}/\text{GaAs}$ quantum dots¹⁹ as well. Thus our calculated diffusion barriers are accurate enough and could be extended to analyze experimental data in bulk and even in nanostructured materials.

Our study can be useful for interpreting more accurately experimental data, especially if taking into account the fact that most experiments for gallium self-diffusion^{49,50} have been performed in n -type or intrinsic material where negatively charged vacancies are more abundant. The most relevant pathway for self-diffusion is the plane-passing mecha-

nism since it has the lowest barrier for diffusion to the second neighbor, while at sufficiently low temperatures diffusion to the first neighbor could be observed for -1 and -2 charge states. By combining information coming from our calculated first and second neighbor diffusion barriers it becomes possible to identify the charge state of the diffusing vacancy in some experiments. For example, in the experiment of Bliss *et al.*,⁴³ V_{Ga} diffuses to the first neighbor by crossing a barrier of 1.1 ± 0.3 eV, which is close to our calculated barrier of 0.84 eV for V_{Ga}^{-1} . In addition, the measured diffusion barrier to the second neighbor is 1.5 ± 0.3 eV, which is comparable to the 1.7 eV we calculated for the -1 charge state. Thus, we can state that diffusing vacancies in this experiment are more probably singly negative instead of the generally accepted triply negative. Recent research works support more and more the hypothesis of a -1 charge state. This was the case, for example, in a recent theoretical study comparing simultaneously the relaxations and lifetimes obtained from simulation and Doppler spectra of positron annihilation experiments; the results confirm the possibility of a -1 charge state for V_{Ga} rather than the -3 charge state.³⁰

V. CONCLUSIONS

The SIESTA-RT approach has been used to study various diffusion pathways for charged gallium vacancies in GaAs, demonstrating that diffusion in bulk semiconductors is a rich and complex phenomenon closely related to the charge state. Different diffusion pathways are identified for negatively charged vacancies, showing that the diffusion process could be nonintuitive and more complex than initially thought. V_{Ga} can diffuse to the second neighbor using two different mechanisms in addition to diffusion to the first and fourth neighbors. Diffusion to the second neighbor is possible by the plane-passing mechanism at all charge states as well as by the previously unrecognized cluster-assisted mechanism, which becomes possible only in the presence of negatively charged vacancies. In addition, gallium vacancy diffusion to the first nearest neighbor is possible only for $q=0, -1, -2$ charges passing by regular or distorted $\text{As}_{\text{Ga}}\text{-X}$ defects. However, this mechanism cannot be considered to be dominant for V_{Ga} since the complete diffusion process was impossible to achieve. Finally, the highest diffusion barrier was recorded for the direct diffusion to the fourth neighbor along the 100 direction for negatively charged vacancies. All barriers for the migration pathways of V_{Ga} are found to increase with increasing numbers of electrons, a behavior opposite to what was recently found in the case of vacancy-mediated self-diffusion in SiC (Refs. 12 and 13) and GaN.^{14,40}

ACKNOWLEDGMENTS

We thank Michel Côté and Vladimir Timochevski for fruitful discussions. N.M. acknowledges partial support from FQRNT (Québec), NSERC (Canada), and the Canada Research Chair program. We thank the RQCHP for generous allocation of computer time.

*Electronic address: f.el.mellouhi@umontreal.ca

†Permanent address: Département de physique and Regroupement québécois sur les matériaux de pointe, Université de Montréal, Case Postale 6128, succ. Centre-ville, Montréal, Québec H3C 3J7, Canada. Electronic address: Normand.Mousseau@umontreal.ca

- ¹Z. M. Wang, S. Seydmohamadi, J. H. Lee, and G. J. Salamo, *Appl. Phys. Lett.* **85**, 5031 (2004).
- ²Z. M. Wang, K. Holmes, J. L. Shultz, and G. J. Salamo, *Phys. Status Solidi A* **202**, R85 (2005).
- ³A. Rastelli, S. Stuffer, A. Schliwa, R. Songmuang, C. Manzano, G. Costantini, K. Kern, A. Zrenner, D. Bimberg, and O. G. Schmidt, *Phys. Rev. Lett.* **92**, 166104 (2004).
- ⁴H. Yu and W. Lu, *Acta Mater.* **53**, 1799 (2005).
- ⁵P. J. Feibelman, *Phys. Rev. Lett.* **65**, 729 (1990).
- ⁶G. Henkelman, G. Jóhannesson, and H. Jónsson, in *Progress on Theoretical Chemistry and Physics*, edited by S. D. Schwartz (Kluwer Academic Publishers, Dordrecht, 2000), pp. 269–300.
- ⁷M. Cogoni, B. P. Uberuaga, A. F. Voter, and L. Colombo, *Phys. Rev. B* **71**, 121203(R) (2005).
- ⁸Y. A. Du, S. A. Barr, K. R. A. Hazzard, T. J. Lenosky, R. G. Hennig, and J. W. Wilkins, *Phys. Rev. B* **72**, 241306(R) (2005).
- ⁹N. Mousseau and G. T. Barkema, *Phys. Rev. E* **57**, 2419 (1998).
- ¹⁰T. F. Middleton and D. J. Wales, *Phys. Rev. B* **64**, 024205 (2001).
- ¹¹M. Bockstedte and M. Scheffler, *Z. Phys. Chem. (Munich)* **200**, 195 (1997).
- ¹²M. Bockstedte, A. Mattausch, and O. Pankratov, *Phys. Rev. B* **68**, 205201 (2003).
- ¹³R. Rurali, E. Hernández, P. Godignon, J. Rebollo, and P. Ordejón, *Comput. Mater. Sci.* **27**, 36 (2003).
- ¹⁴S. Limpijumngong and C. G. Van de Walle, *Phys. Rev. B* **69**, 035207 (2004).
- ¹⁵I. V. Ionova and E. A. Carter, *J. Chem. Phys.* **98**, 6377 (1993).
- ¹⁶C. Corbel, F. Pierre, K. Saarinen, P. Hautojärvi, and P. Moser, *Phys. Rev. B* **45**, 3386 (1992).
- ¹⁷H. Bracht and S. Brotzmann, *Phys. Rev. B* **71**, 115216 (2005).
- ¹⁸F. Tuomisto, K. Pennanen, K. Saarinen, and J. Sadowski, *Phys. Rev. Lett.* **93**, 055505 (2004).
- ¹⁹H. S. Djie, O. Gunawan, D.-N. Wang, B. S. Ooi, and J. C. M. Hwang, *Phys. Rev. B* **73**, 155324 (2006).
- ²⁰T. Raz, N. Shuall, G. Bahir, D. Rittera, D. Gershoni, and S. N. G. Chu, *Appl. Phys. Lett.* **85**, 3578 (2004).
- ²¹D. Sánchez-Portal, P. Ordejón, E. Artacho, and J. M. Soler, *Int. J. Quantum Chem.* **65**, 453 (1997).
- ²²R. Malek and N. Mousseau, *Phys. Rev. E* **62**, 7723 (2000).
- ²³F. Valiquette and N. Mousseau, *Phys. Rev. B* **68**, 125209 (2003).
- ²⁴G. Wei, N. Mousseau, and P. Derreumaux, *J. Chem. Phys.* **117**, 11379 (2002).
- ²⁵F. El-Mellouhi, N. Mousseau, and P. Ordejón, *Phys. Rev. B* **70**, 205202 (2004).
- ²⁶N. Troullier and J. L. Martins, *Phys. Rev. B* **43**, 1993 (1991).
- ²⁷L. Kleinman and D. M. Bylander, *Phys. Rev. Lett.* **48**, 1425 (1982).
- ²⁸F. El-Mellouhi and N. Mousseau, *Phys. Rev. B* **71**, 125207 (2005).
- ²⁹D. J. Chadi, *Mater. Sci. Semicond. Process.* **6**, 281 (2003).
- ³⁰I. Makkonen, M. Hakala, and M. J. Puska, *Phys. Rev. B* **73**, 035103 (2006).
- ³¹J. A. Van Vechten, *J. Phys. C* **17**, L933 (1984).
- ³²P. E. Blöchl, E. Smargiassi, R. Car, D. B. Laks, W. Andreoni, and S. T. Pantelides, *Phys. Rev. Lett.* **70**, 2435 (1993).
- ³³J. Dabrowski, *Diffus. Defect Data, Pt. B* **B71**, 23 (2000).
- ³⁴G. Henkelman, B. P. Uberuaga, and H. Jónsson, *J. Chem. Phys.* **113**, 9901 (2000).
- ³⁵F. Wooten, K. Winer, and D. Weaire, *Phys. Rev. Lett.* **54**, 1392 (1985).
- ³⁶D. J. Chadi, *Phys. Rev. B* **68**, 193204 (2003).
- ³⁷H. Overhof and J.-M. Spaeth, *Phys. Rev. B* **72**, 115205 (2005).
- ³⁸T. Steinegger, B. Gründig-Wendrock, M. Jurisch, and J. R. Niklas, *Physica B* **308-310**, 745 (2001).
- ³⁹V. Bondarenko, J. Gebauer, F. Redman, and R. Krause-Rehberg, *Appl. Phys. Lett.* **87**, 161906 (2005).
- ⁴⁰M. G. Ganchenkova and R. M. Nieminen, *Phys. Rev. Lett.* **96**, 196402 (2006).
- ⁴¹F. El-Mellouhi and N. Mousseau, *J. Appl. Phys.* **100**, 083521 (2006).
- ⁴²G. Lengel, J. Harper, and M. Weimer, *Phys. Rev. Lett.* **76**, 4725 (1996).
- ⁴³D. E. Bliss, W. Walukiewicz, and E. E. Haller, *J. Electron. Mater.* **22**, 1401 (1993).
- ⁴⁴J. L. Rouviere, Y. Kim, J. Cunningham, J. A. Rentschler, A. Bourret, and A. Ourmazd, *Phys. Rev. Lett.* **68**, 2798 (1992).
- ⁴⁵R. Geursen, I. Lahiri, M. Dinu, M. R. Melloch, and D. D. Nolte, *Phys. Rev. B* **60**, 10926 (1999).
- ⁴⁶D. E. Bliss, W. Walukiewicz, J. W. Ager, E. E. Haller, K. T. Chan, and S. Tanigawa, *J. Appl. Phys.* **71**, 1699 (1992).
- ⁴⁷I. Lahiri, D. D. Nolte, M. R. Melloch, J. Woodall, and W. Walukiewicz, *Appl. Phys. Lett.* **69**, 239 (1996).
- ⁴⁸S. Balasubramanian, S. W. Mansour, M. R. Melloch, and D. D. Nolte, *Phys. Rev. B* **63**, 033305 (2001).
- ⁴⁹B. Bracht, M. Norseng, E. E. Haller, K. Eberl, and M. Cardona, *Solid State Commun.* **112**, 301 (1999).
- ⁵⁰J. Gebauer, M. Lausmann, F. Redmann, R. Krause-Rehberg, H. S. Leipner, E. R. Weber, and P. Ebert, *Phys. Rev. B* **67**, 235207 (2003).